JOURNAL OF
THE INTERNATIONAL ASSOCIATION
FOR SHELL AND SPATIAL
STRUCTURES

FORMERLY BULLETIN OF THE INTERNATIONAL ASSOCIATION FOR SHELL AND SPATIAL STRUCTURES

Prof. D. h-C Eng .E. TORROJA, founder

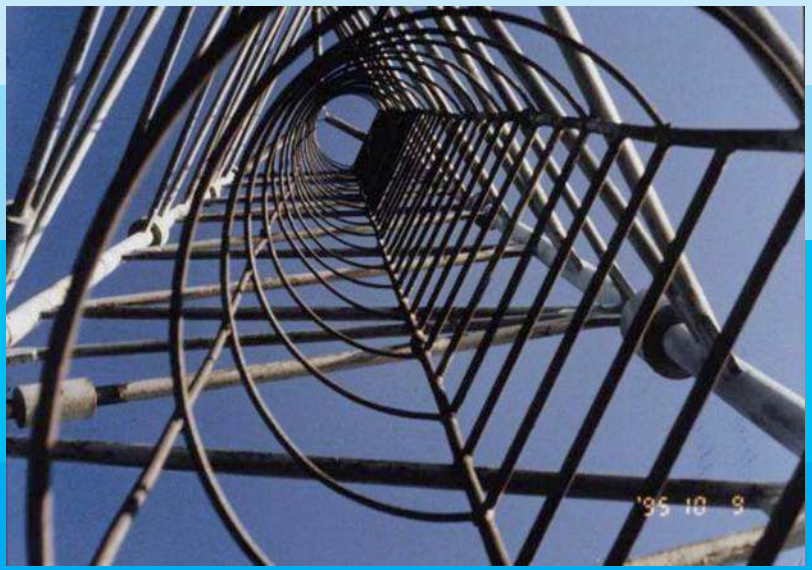

SPECIAL ISSUE

MASTS AND TOWERS *Part 1*

Guest Editor: **U. STØTTRUP-ANDERSEN**

Vol. 55 (2014) No. 2

June n. 180

ISSN: 1028-365X

Journal

VOL. 55 (2014) No. 2
n. 180 June

contents

COVER: *Figure from paper by U. Stottrup-Andersen*

IASS Secretariat: CEDEX-Laboratorio Central de Estructuras y Materiales
Alfonso XII, 3; 28014 Madrid, Spain
Tel: 34 91 3357409; Fax: 34 91 3357422; iass@cedex.es; http://www.iass-structures.org

Printed by SODEGRAF ISSN:1028-365X Depósito legal: M. 1444-1960

FULL-SCALE MEASUREMENTS OF TOWERS AND MASTS AND COMPARISON WITH THEORETICAL SIMPLIFIED ANALYSIS

Jiří LAHODNÝ[1], Vladimír JANATA[1]

[1]Ph.D., Eng., EXCON a. s., Sokolovská 187/203, 190 00 Prague, lahodny@excon.cz, janata@excon.cz

Editor's Note: Manuscript submitted 5 December 2013; revision received 25 March 2014; accepted 14 June. This paper is open for written discussion, which should be submitted to the IASS Secretariat no later than December 2014.

ABSTRACT

The wind action and response of towers and masts to turbulent wind are described in the paper. The results of full-scale measurements carried out on one tower and one guyed mast are presented. The measured characteristics, especially the power spectral densities of the wind velocities and the structure response, are compared with theoretical presumptions. The measured structures are situated in different terrains. Subsequently, a practical method for the theoretical evaluation of the structure response to turbulent wind is proposed. The method, based on the spectral analysis approach, takes into account the contribution of all significant mode shapes. The method can be used for a wide range of towers and masts, especially for those which do not meet EN standards criteria for commonly used equivalent static methods.

***Keywords*:** *Full-scale measurement, tower, mast, spectral analysis, simplified spectral analysis*

1. INTRODUCTION

The paper focuses on wind loading and the theoretical determination and measurement of structure response. The different methods for theoretical analysis were studied particularly with respect to their practical application with new European standards. The measurement was used to compare theoretical and measured responses as well as to investigate the suitability of the wind characteristics recommended by European standards, especially for the region of the Czech Republic.

The authors carried out several full-scale measurements on towers and masts in recent years in the Czech Republic. The first measurements were performed with the aim of determining the proper dynamic characteristics of the structures, the efficiency of dampers and/or local wind characteristics for the more accurate assessment of existing TV broadcasting towers and masts. To obtain relevant and more general conclusions, the full-scale measurements were extended in the second phase. More sensors were installed for longer periods. These measurements and research are realized with support from the Ministry of Industry and Trade of the Czech Republic. The main goal of the measurements is to collect data for evaluating wind properties in the Czech Republic and to compare the theoretically expected behaviour of the structures with the measured behaviour. Two measurements are described in the paper.

2. THEORETICAL ANALYSIS

The wind action and also the structure response have a strong random character caused particularly by wind turbulence. The properties of the wind and the structure response are therefore advantageously described using statistical variables and statistical functions in the frequency domain such as the power spectral densities and the coherence function. Subsequently, the theory of stochastic processes is used for the theoretical evaluation of the structure response [1].

The wind velocity and, similarly, the structure response are usually divided into the mean and the fluctuation component, which is expressed using the standard deviation. For the maximum values of the fluctuation component, the peak factors are derived [2]. This can be written for wind velocities as

$$v_{\max}(z) = v_m(z) + v_{fl}(z) = v_m(z) + k_v \cdot \sigma_v \qquad (1)$$

Copyright © 2014 by Jiří LAHODNÝ, Vladimír JANATA.
Published by the International Association for Shell and Spatial Structures (IASS) with permission.

where v_{max} and v_m are the maximum and the mean wind velocities, σ_v the standard deviation and k_v the peak factor of the wind velocity. Similarly for the response it may be written

$$u_{\max}(z) = u_m(z) + u_{fl}(z) = u_m(z) + k_p \cdot \sigma_u(z) \qquad (2)$$

where u_{max} and u_m are the maximum and the mean response, σ_u the standard deviation and k_p the peak factor of the structure response.

The mean component of the structure response can be solved by static calculation. The fluctuation component results from statistical analysis, detailed description, e.g. [3]. The standard deviation can be determined as

$$\sigma_{u_i}^2 = \int_0^\infty S_{u_i u_i}(f) \cdot df \qquad (3)$$

where $S_{u_l u_l}(f)$ is the power spectral density of the response and f stands for the frequency. The peak factor is defined as

$$k_p = \sqrt{2 \cdot \ln(\nu \cdot T)} + \frac{0{,}5772}{\sqrt{2 \cdot \ln(\nu \cdot T)}} \qquad (4)$$

where T is the integration period of random process and ν the up-crossing frequency expressed by Eq. (5)

$$\nu = \sqrt{\frac{\int_f f^2 \cdot S_{uu}(f) \cdot df}{\int_f S_{uu}(f) \cdot df}} \approx \sqrt{\frac{\sum_k f_k^2 \, {}^R\sigma_{k,u_l}^2}{{}^B\sigma_{u_l}^2 + \sum_k {}^R\sigma_{k,u_l}^2}} \qquad (5a,5b)$$

where ${}^B\sigma_u$ represents the standard deviation of the background response and ${}^R\sigma_{k,u}$ of the resonant response of k^{th} mode shape.

The simple expression is used for the response power spectral density determination:

$$S_{u_l u_l}(f) = \sum_i \sum_j H_{u_l F_i}(if) \cdot H_{u_l F_j}^*(if) \cdot S_{F_i F_j}(f) \qquad (6)$$

The function $S_{u_l u_l}(f)$ represents the power spectral density of the fluctuation response in point l and $S_{F_i F_j}(f)$ is the power spectral density of fluctuation load of points i and j. $H_{u_l F_i}(if)$ is the frequency characteristic describing the relationship between random load F_i (in point i) and the response u_l (in point l). $H_{u_l F_j}^*(if)$ stands for the complex conjugate of $H_{u_l F_j}(if)$. The power spectral density of load is determined as

$$S_{F_i F_j}(f) = \rho^2 \cdot v_{m,i} \cdot v_{m,j} \cdot c_{W,i} \cdot c_{W,j} \cdot A_i \cdot A_j \cdot \chi_i(f) \cdot \chi_j(f) \cdot \sqrt{S_{v_i v_i}(f)} \cdot \sqrt{S_{v_j v_j}(f)} \cdot coh_{i,j}(f) \qquad (7)$$

where ρ is the air density, $v_{m,i}$ and $v_{m,j}$ the mean wind velocities in points i and j, the product $c_{w,i} \cdot A_i$ the wind drag in point i, $\chi_i(f)$ the aerodynamic admittance for projected area appropriate to point i. $S_{v_i v_i}(f)$ represents the power spectral density of the wind velocity in point i and $coh_{i,j}(f)$ the coherence function for points i and j.

Decomposition into the mode shapes method can be used to derive the frequency characteristic functions [3], which can be then written as

$$H_{u_l P_j}(if) = \sum_k \frac{\phi_{k,i} \cdot \phi_{k,j}}{m_k \cdot 4\pi^2 (f_k^2 - f^2 + 2i\xi_k f_k f)} \qquad (8)$$

where m_k means the generalized mass, f_k the natural frequency, ξ_k the damping ratio of k^{th} mode, $\phi_{k,i}$ and $\phi_{k,j}$ are the mode shape values in points i and j.

3. SIMPLIFIED THEORETICAL ANALYSIS

The simplified methods are mainly used in design practice. The dynamic problem is mostly converted to a static one using the dynamic or gust factor. The quasi-static or equivalent static methods are used in many standards, including the Eurocodes and TIA/EIA. These methods are sufficiently accurate for most towers and masts. But very slender ones and/or structures with atypically distributed masses, structure rigidity or wind drag should be analyzed using more exact methods. The full spectral analysis described in the previous chapter or analysis in the time domain, see e.g. [4], can be used. Alternatively, other simplified methods are also available and suitable in these cases, namely the method using influence lines proposed by Davenport, described in e.g. [5] or the other approaches, for example [6, 7]. These methods were

studied with the aim of finding the most suitable approach for the practical design of the structures in accordance with the EN standards requirements and wind characteristics.

Subsequently, another variant was proposed and is presented in this paper. This approach follows the main principles of the Davenport statistic method, but takes advantage of the current software used in design practice, e.g. the possibility of determining deflections as well as the internal forces of mode shapes. An alternative simplified solution of the standard deviations of the background and the resonant components of response is suggested [8]. Ordinary software used in engineering practice is sufficient for their evaluation. The approach is harmonious with new EN standards and can be useful and practical for some kinds of structures.

The following commonly used simplifications were applied for the derivation of this approach. The background and the resonant response are solved separately. The resonant response appropriated to certain mode shape is analysed for the constant power spectral density of load. The low damping of the structure is assumed. The background response caused by variable action without influence by inertia forces of resonant vibration is solved using static calculation with regard to the fact that this part of the response represents "slow" motion of the structure.

3.1 Standard deviation of the resonant response

The standard deviation of the resonant response related to k^{th} mode shape, denoted ${}^{R}\sigma_k$, is stated as directly proportional to the mode shape ϕ_k

$$ {}^{R}\sigma_k = q_k \cdot \phi_k \tag{9}$$

Parameter q_k is derived as

$$ q_k = \left(\frac{1}{64 \cdot \pi^3 \cdot m_k^2 \cdot f_k^3 \cdot \xi_k} \sum_i \sum_j \phi_{k,i} \cdot \phi_{k,j} \cdot S_{F_i F_j}(f_k) \right)^{0.5} \tag{10}$$

where ${}^{R}\sigma_k$ is the standard deviation of the resonant response of k^{th} mode, m_k is the generalized mass, f_k stands for the natural frequency, ξ_k the damping ratio of k^{th} mode, $\phi_{k,i}$ and $\phi_{k,j}$ are the mode shape values at points i and j, $S_{F_i F_i}(f_k)$ implies the spectral density of fluctuation load in points i and j defined by Eq. (7).

This follows directly from Eqs. (3, 6 and 8) when the constant load power spectral density is assumed. Then it can be written

$$ {}^{R}\sigma^2_{k,u_l} = \int_0^\infty {}^{R}S_{u_l u_l}(f) \cdot df = \phi^2_{k,l} \cdot \left(\frac{1}{64 \cdot \pi^3 \cdot m_k^2 \cdot f_k^3 \cdot \xi_k} \cdot \sum_i \sum_j \phi_{k,i} \cdot \phi_{k,j} \cdot S_{F_i F_j}(f_k) \right) \tag{11}$$

where ${}^{R}\sigma_{k,u_l}$ is the standard deviation of the resonant response in point l appropriated to k^{th} mode shape, and ${}^{R}\phi_{k,l}$ is value of k^{th} mode shape in point l. The expression in the parentheses is a constant number for the given mode shape and can be made equal to the square value of the desired parameter q_k. The parameter is the same for both the deflections and internal forces and may be used for scaling the dimensionless mode shape to the resultant shape of the standard deviation of the resonant response.

The described evaluation of the resonant part of the response can be used for towers as well as for guyed masts (if resonant vibration around a mean equilibrium position of the masts is assumed to be linear).

3.2 Standard deviation of the background response

The standard deviation of the background response is determined using static calculation for loads

$$ F_{fl,\sigma_B}(z) = F_m(z) \cdot 2 \cdot I_v(z) \cdot \sqrt{B^2(h_s, b_s)} \tag{12}$$

where z is the height above the ground, I_v the intensity of turbulence, F_m the mean load and $B^2(h_s,b_s)$ is the background factor according to [9] for the height and width of the part of the structure impacted by wind gust. Eq. (12) is implied from equation (6.2) in [9] and respects the lack of full correlation of the wind load on the related part of the structure.

Generally, several load cases with different load location and its length should be applied to obtain maximal values of the background response in all members and levels of the tower. The most accurate

results will be obtained if an individual load case is taken for each elevation at which assessment is required. These load patterns are depicted in Fig. 1.

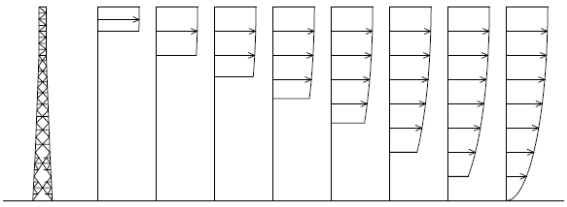

Figure 1: *Example of load case group for background response determination of tower according to Eq. (12)*

A comparative analysis proved that if only one load case is considered (load on the whole height) in the case of ordinary towers with a height of about 40 m, the inaccuracy of the total response will be less than 3% in comparison with the response calculated using a full group of the load cases according to Fig. 1, see [8].

The described evaluation of the background part of the response is suitable for towers only. The background response of the guyed mast should be determined using the patch load method [10, 11] with appropriate peak factors. The patch load method can be used for the evaluation of the background response even in the case criteria for the overall response determination using this approach are not met, see [11]. When Eqs. (9, 10) are used for the resonant response and the patch load method for the background response of guyed masts, it is possible to analyse a wide range of guyed masts which do not meet the criteria for equivalent static methods in accordance with EN standards recommendations and requirements.

For the guyed masts that do not significantly meet the patch load method criteria or for the investigation of the background response an alternative solution of background response determination can be used in a similar but more complex manner as for the towers. The group of load patterns is used for nonlinear static loading of the mast. Nonlinear behaviour of the structure is thus respected for the evaluation of the background response, which is an advantage compared to linear analysis in the frequency domain. On the other hand, many load cases must be taken into account for relevant response determination. The numerical simulation of wind load is advantageously used for the generation of load cases. Examples of two simulated load cases are depicted in Fig. 2. The numerical simulation method, e.g. according to Iwatani, can be performed [12]. The Iwatani simulation proves to be very effective, with very good agreement between the simulated and required wind turbulent characteristics. The background response of the structure is subsequently solved using nonlinear static analysis for all load cases composed of the mean wind load + simulated fluctuation load. Thus, the approach is analogous to analysis in the time domain, see e.g. [4]. But only nonlinear static analysis is used and there are much fewer requirements for the mathematical modelling of the structure and calculation. The difference between the results of static and dynamic time domain analysis is apparent in Fig. 3. The resultant background part of the response is then stated as the difference between the resultant total response and the mean wind response.

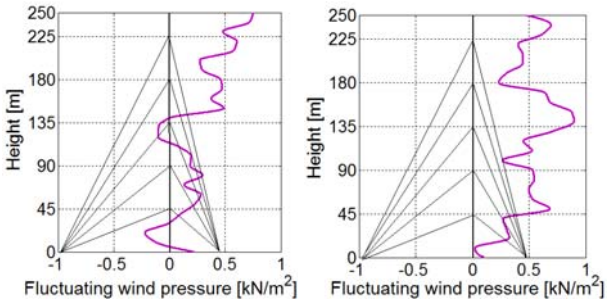

Figure 2: *Example of two load cases for background response determination of guyed masts. Fluctuation wind pressure is depicted (without mean wind component)*

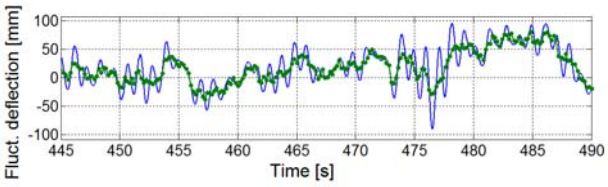

Figure 3: *Example of the response to simulated wind action. Green points are the results of the static calculation of load case series and represent the background response component. The blue line is the result of the time domain analysis for the same load time history and represents the overall fluctuation response of the structure*

The total number of load cases corresponds to the time integration period. For example, for a ten-minute period and simulated load cases for each 0.2 s, 3000 load cases will be taken into calculation.

The analysis should be done for several simulated groups of load cases and the resultant maxima, minima or standard deviations of the background response are stated as average values of maxima, minima or standard deviations of these groups of results.

3.3 Standard deviation of overall response

Finally, if the standard deviations are known, the overall response is determined according to Eq. (2) for the total standard deviation of the response σ_{u_l} equal to

$$\sigma_{u_l} = \sqrt{{}^{B}\sigma_{u_l}^2 + \sum_k {}^{R}\sigma_{k,u_l}^2} \qquad (13)$$

and for the peak factor according to Eqs. (4, 5b) [5].

4. FULL-SCALE MEASUREMENT

4.1 Description of measured structures

Two examples of full-scale measurements are presented. The first one was carried out on the Praděd tower, the second one on guyed mast at Javořice, see Fig. 4.

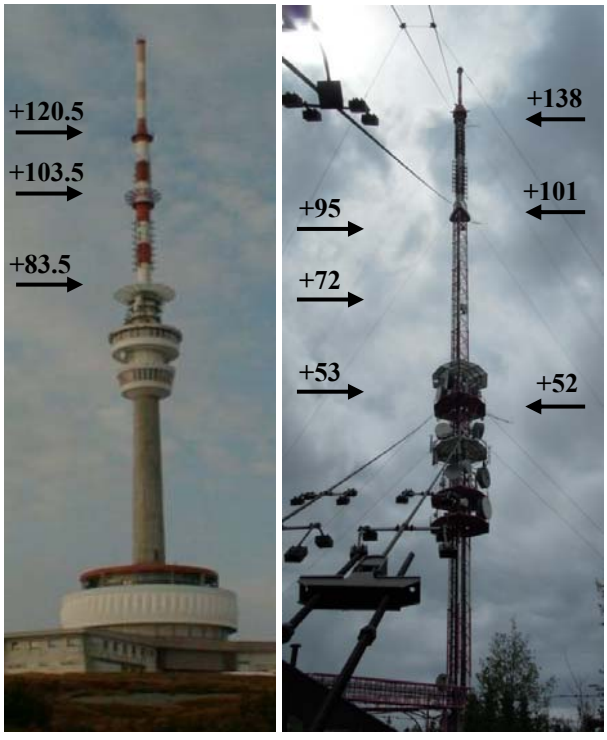

Figure 4: *Praděd tower and the guyed mast at Javořice, elevations of sensors*

4.1.1 Praděd tower

The tower with a height of 146 m consists of concrete, steel and a GRP part, see Fig. 4. The height of the tubular concrete part is 88.4 m, the diameter narrows from 6.5 to 5 m. The steel part with a height of 40.5 m is tubular with a diameter of 3 m. The GRP extension with a diameter of 1.93 m is 22 m tall. A pendulum damper with a weight of about one ton is placed at the top to eliminate oscillation due to vortex shedding. The damper is tuned to the second natural frequency 1.02 Hz, on which the vortex shedding vibration could reach critical amplitudes. The damper influence on damping of the first mode shape (with frequency 0.46 Hz) is supposed to be minor. The short term measurement was performed on this tower. The accelerometers were placed at three elevations – 83.5, 103.5 and 120.5 m. The wind velocity was measured simultaneously at one level at the height of 103.5 m. The response during very strong wind conditions was recorded.

4.1.2 Guyed mast at Javořice

The guyed mast at Javořice consists of a triangular lattice shaft and a slender cantilever. Three guyed levels are at the heights of 48.5, 100 and 137 m. The overall height of the structure is 163.5 m. The height of the cantilever is 25.5 m. The liquid damper with a weight of about one ton is placed at the top to eliminate oscillation due to vortex shedding. The damper is tuned to mitigate oscillation in the range from 1.7 to 6.6 Hz, where vortex shedding vibration could reach critical amplitudes. The damper influence on damping of the first 8 mode shapes (with frequencies under 1.7 Hz) is supposed to be negligible. The criteria for patch load method [11] are not met (the height of the cantilever is higher than half of the span under the top guy level). There are also significant differences in rigidity and wind drag along the height, see Fig. 4.

The full-scale measurement was performed with the following placement of sensors. Three anemometers were placed at levels 52, 101 and 138 m above the ground. The pairs of accelerometers were installed at the same levels. Strain gauges were mounted at three levels – 53, 71.5 and 95.4 m (i.e. in the upper and lower end of the span and in the middle) on the legs. Later, the strain gauges were also placed at the foot of the cantilever. Other strain gauges were glued on the tensioning rods of guy cables.

4.2 Measurement of wind characteristics

The wind velocity and direction were measured using ultrasonic anenometers at several elevations. The decomposition of the velocity into longitudinal and lateral components was carried treating the wind velocity vectors as complex numbers and considering Fig. 5. Along-wind and cross-wind velocity components are determined from the following relationships:

$$v_{\text{fl,long}} = |\vec{v}_{\text{fl},i}| \cdot \cos(\alpha_{\text{fl},i}) \tag{14a}$$

$$v_{\text{fl,lat}} = |\vec{v}_{\text{fl},i}| \cdot \sin(\alpha_{\text{fl},i}) \tag{14b}$$

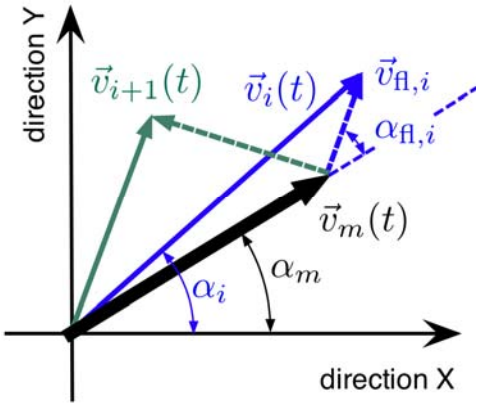

Figure 5: *Decomposition of the wind velocity into its mean and fluctuating parts and consequently into the lateral and longitudinal components*

The power spectral densities of wind velocity obtained from measurement were compared with theoretical ones. The four theoretical spectra were chosen for the comparison:

Kármán spectrum [13]:

$$\frac{f \cdot S_v(f)}{v_*^2} = \frac{4 \cdot \beta \cdot f_L(f)}{\left(1 + 70.8 \cdot f_L^2(f)\right)^{5/6}} \tag{15a}$$

$$\text{where } f_L(f) = \frac{f \cdot L}{v_m} \tag{15b}$$

Davenport spectrum [14]:

$$\frac{f \cdot S_v(f)}{v_*^2} = 4.0 \cdot \frac{f_L^2(f)}{\left(1 + f_L^2(f)\right)^{4/3}} \tag{16a}$$

$$\text{where } f_L(f) = \frac{1200 \cdot f}{v_m(10)} \tag{16b}$$

Kaimal spectrum [15]:

$$\frac{f \cdot S_v(z,f)}{v_*^2} = \frac{200 \cdot f_L(z,f)}{\left(1 + 50 \cdot f_L(z,f)\right)^{5/3}} \tag{17a}$$

$$\text{where } f_L(z,f) = \frac{f \cdot z}{v_m(z)} \tag{17b}$$

Eurocode spectrum [9]:

$$\frac{f \cdot S_v(z,f)}{v_*^2} = \frac{\beta \cdot 6.8 f_L(z,f)}{\left(1 + 10.2 f_L(z,f)\right)^{5/3}} \tag{18a}$$

$$\text{where } f_L(z,f) = \frac{f \cdot L(z)}{v_m(z)} \tag{18b}$$

The quantity L in the Eq. (15-18) represents the turbulent length scale, v_* the shear wind velocity, v_m the mean wind velocity and z the height above the ground. Factor β stands for the relationship between the standard deviation of the wind velocity and the shear wind velocity $\beta = \sigma_v^2 / v_*^2$.

The non-dimensional spectra (right sides of Eq. (15-18) as well as the power spectral densities of wind velocities $S_v(f)$ were compared. Typical results are shown in Figs. 6-8. The measurement was performed on the 164 m guyed mast at Javořice, see 4.1.2. The guyed mast is situated in forested terrain, but the terrain changes from the smoother terrain at a distance of approximately 8 km in the upwind direction.

The higher wind velocities must be chosen for the evaluation of the spectral densities. The results obtained from lower wind velocity records give usually unsteady and unreliable results.

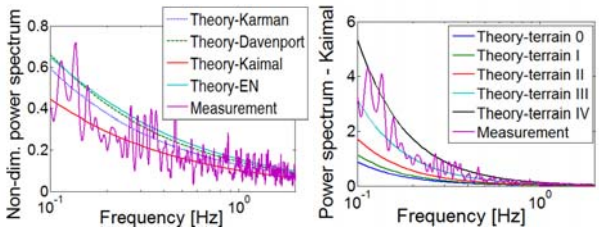

Figure 6: *The comparison of measured and theoretical non-dimensional spectra (left side). The comparison of measured spectrum and theoretical Kaimal spectrum for different terrain roughness (right side). Guyed mast at Javořice, height of anemometer 52 m, mean wind velocity 10.6 m/s*

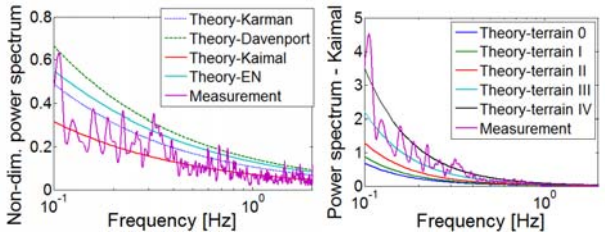

Figure 7: *The comparison of measured and theoretical non-dimensional spectra (left side). The comparison of measured spectrum and theoretical Kaimal spectrum for different terrain roughness (right side). Guyed mast at Javořice, height of anemometer 101 m, mean wind velocity 11.9 m/s*

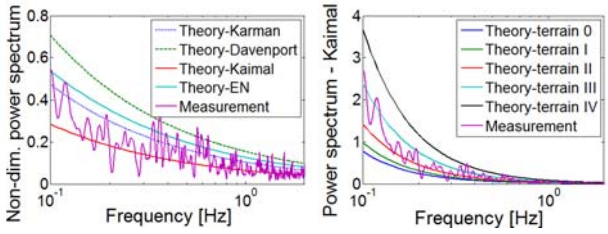

Figure 8: *The comparison of measured and theoretical non-dimensional spectra (left side). The comparison of measured spectrum and theoretical Kaimal spectrum for different terrain roughness (right side). Guyed mast at Javořice, height of anemometer 138 m, mean wind velocity 13.7 m/s*

The good agreement between the measured spectrum and Kaimal spectrum is noticeable in Figs. 6-8. Similar agreement was apparent at most of the measured sites. For these sites the Eurocode spectrum seems to be conservative. But in some other cases, the measured spectrum was higher and closer to the Eurocode spectrum.

The measured power spectral densities correspond closely to the terrain roughness. The influence of the transition between roughness categories is apparent in Figs. 6-8. The wind properties obtained from two lower anemometers correspond to closer forested terrain, the wind properties at the height of the third anemometer correspond to more distant open terrain. The height where the turbulent wind properties are changing due to terrain roughness transition corresponds more to an expression according to [2] than EN standards [9], Annex A, Procedure 2, which seems to be very conservative.

The limited number of the measurements and the necessity of higher wind speed recording does not currently allow the reliable recommendation of the spectral densities for the region of the Czech Republic generally, but it is obvious that measurement can bring more accurate wind characteristics and be useful, for example, for the assessment of existing towers and masts.

4.3 Measurement of structure response

The sensors were placed on the structures at several levels. Acceleration was usually measured at three levels by Endevco 86 accelerometers. Two accelerometers set perpendicular to one other were placed at measured elevations to record the response in both horizontal directions. Simultaneously, strain measurement was carried out using strain gauges mounted on the shaft and on the stretching rods of the guys.

5. COMPARISON OF THE RESPONSE

The structure response to wind action is influenced by many factors such as the wind drag of the structure, damping, the height profile of mean wind velocity and others. The number of these factors and their uncertainties can cause significant differences between theoretical analysis and the real state. The full-scale measurement can give information about this difference in the given investigated case. Despite the unknown inaccuracy of input parameters of the theoretical analysis, the comparison of the theoretical results with the full-scale measurement can verify the suitability of the chosen computation method. The character of the structure behaviour and the importance of each individual response component can be investigated.

5.1 Praděd tower

First, a comparison of the results of several theoretical approaches was performed and is depicted in the Fig. 9.

The slenderness and low rigidity of the extension together with heavy discrete mass near the top (part with damper) leads to the significant growth of the resonant component of response at non-damped natural frequencies.

The quasi-static method according to the EN standard [9] thus underestimated internal forces in fibre-glass extension, as is apparent in Fig. 9. The results of the simplified method according to chapter 3 were subsequently compared with non-simplified spectral analysis according to chapter 2 and with the method using influence lines [5] by

Davenport et al. The very good agreement between the results of these methods was observed. The relatively low impact of the number of load cases for background response evaluation according to Fig. 1 on the overall response is visible in Fig. 9. The different way of computation did not make it possible to use exactly the same expression of correlation of the wind load for the determination of the background response using influence lines method. The minor difference between Davenport and the other results (except the red line) is caused mainly by this variance.

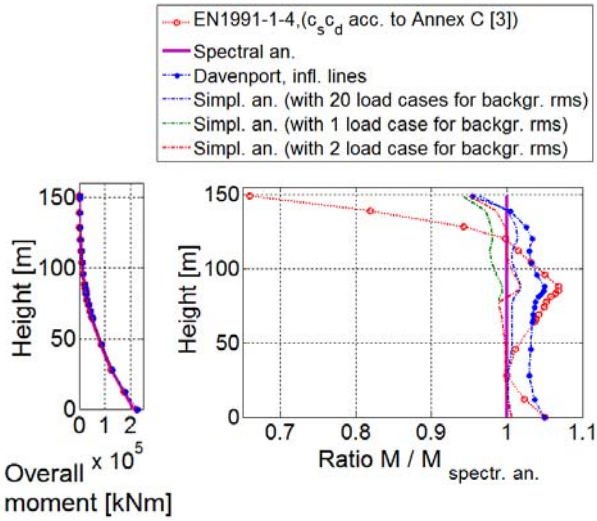

Figure 9: *Left: Overall moments. Right: Ratios of the moments according to various methods to the moment resulting from spectral analysis described in section 2*

Subsequently, measured resonant response was compared with the theoretical one. Time history records of acceleration were numerically integrated to obtain the velocity and the deflection time history. The calculation was carried out for an integration time period 60 s, which corresponds to the measured length of the records. The wind properties and the wind profile were assumed according to [9] for terrain roughness II.

Table 1: *Maximum, minimum and standard deviation of the resonant response – overview of measured (left) and theoretical values (right), record A*

Measurement - record A

Sensor elevation	Resonant deflection [mm]		
	min	max	standard deviation
120.5 m	-41.8	40.0	15.7
103.5 m	-26.8	25.9	10.3
83.5 m	-19.0	19.0	7.4

Theory for v_m =29 m/s at level 103.5m, terrain category II and T = 60s

Sensor elevation	Resonant deflection [mm]		
	min	max	standard deviation
120.5 m	-35.0	35.0	12.5
103.5 m	-24.9	24.9	8.9
83.5 m	-15.0	15.0	5.4

Table 2: *Maximum, minimum and standard deviation of the resonant response – overview of measured (left) and theoretical values (right), record B*

Measurement - record B

Sensor elevation	Resonant deflection [mm]		
	min	max	standard deviation
120.5 m	33.1	32.4	12.7
103.5 m	-22.8	21.8	8.5
83.5 m	-15.0	16.0	6.0

Theory for v_m =28 m/s at level 103.5m, terrain category II and T = 60s

Sensor elevation	Resonant deflection [mm]		
	min	max	standard deviation
120.5 m	-31.9	31.9	11.4
103.5 m	-22.8	22.8	8.1
83.5 m	-13.7	13.7	4.9

The numerical comparison of the theoretical and measured resonant response is shown in Tabs. 1 and 2. The horizontal deflections are compared. Good agreement was found.

5.2 Guyed mast at Javořice

The comparison of different theoretical approaches as well as the comparison between theoretical and measured responses was carried out. The presented response was recorded at the same time as the wind properties described in chapter 4.2. Deflections at levels 49, 98 and 138 m were calculated from the time history of acceleration. The measured time history of the strain in the legs was converted to the stresses and the axial forces. The moments in the shaft were determined from the axial leg forces. The overall measured standard deviations of the response were subsequently divided into two components to be compared with theoretical values of the background and the resonant standard deviations. The separation of components was carried out using power spectral densities of the bending moments, see Fig. 10. The individual standard deviations were stated numerically as the areas under the density curve in the related frequency intervals. Although this is not strictly theoretically correct, the accuracy of the resultant value is sufficient for comparison purposes.

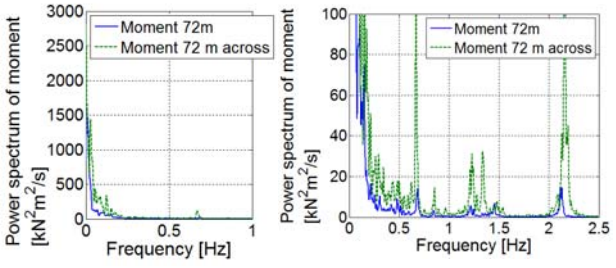

Figure 10: *Power spectral density of bending moments in the shaft at the level of 72 m. The spectra of the moments in both directions are depicted. The left and right side of the figure represent the same spectrum, but the vertical scale was magnified on the right side to make the resonant part more visible*

A significant response in the lateral direction is apparent in Fig. 10 (direction of the wind was approximately parallel to the direction of guys during the measurement).

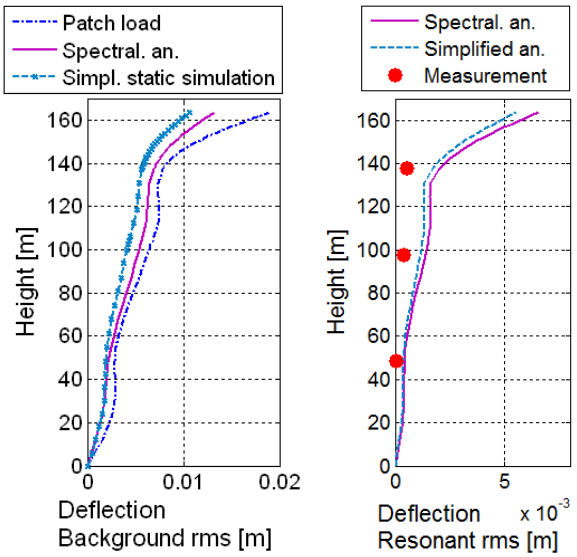

Figure 11: *Standard deviations of background (left) and resonant (right) horizontal deflections. Comparison of theoretical results and measurements*

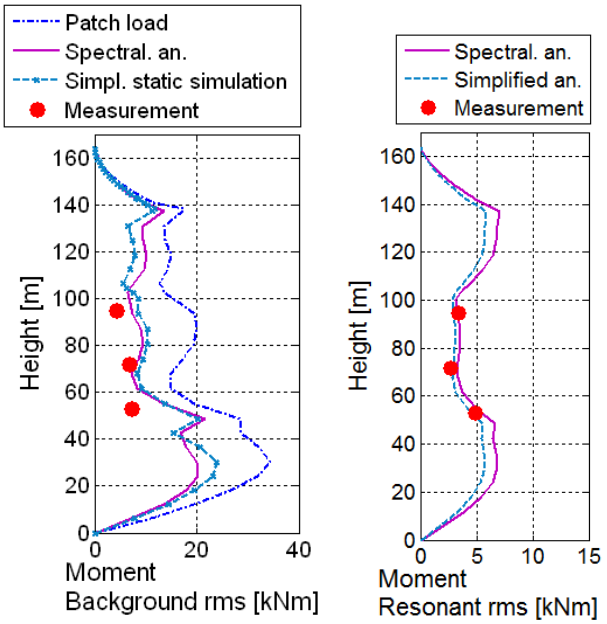

Figure 12: *Standard deviations of background (left) and resonant (right) bending moments. Comparison of theoretical results and measurements*

The results of theoretical approaches are compared to the measured values of the response. The calculations were carried out for the measured velocities and the wind properties, see chapter 4.2.

The results of the analysis described in chapter 2 (denoted as "Spectral an.") together with the results of the simplified approach according to chapter 3.1 (denoted as "Simplified an.") for the resonant part and according to chapter 3.2 (denoted as "Simpl. static simulation") for the background part are presented in Figs. 11 and 12. Standard deviations of horizontal deflection and bending moments are depicted.

The results of the patch load method according to [11] for the background response are also presented. The standard deviations of the background response calculated using [10, 11] follow the shape of the other depicted results, but are higher. As the parameters for the patch load method were derived for strong wind conditions, the results of methods cannot be reliably compared. Nevertheless, the suitability of the patch load method for the background response determination of guyed mast, which does not meet the method criteria, can be seen in this case. The good agreement is apparent between measured and theoretic values of moments. The measured resonant horizontal deflection is lower compared to theory.

6. CONCLUSIONS

The simplified approach for the determination of tower and mast response to the turbulent wind is suggested in the paper. The approach is applicable to the structures with the general geometry, general distribution of masses and areas exposed to the wind and with the general (low) damping. It is harmonised with EN standards and can be used for structures that do not meet criteria for the commonly used equivalent static method.

The results of two full-scale measurements have been presented. Theoretical expectations of the structure behaviour were compared with the results of measurements. Although there are many factors influencing the response of the structure, the agreement between the measured and the theoretical values of the response was found to be very good in both cases. It generally confirms the suitability of approaches being used for the design of towers and masts.

The measurement of power spectral densities of the wind velocities typically shows better agreement with Kaimal spectrum. The relationship between the distance from the roughness transition and the

height where wind properties change shown in [9] seems to be very conservative compared to the results of measurement. The significant lateral response was observed in the case of guyed mast measurements.

The next full-scale measurement will be carried out in the near future to improve knowledge of the real response of masts and towers to gusty wind.

7. ACKNOWLEDGEMENTS

The full-scale measurements and data evaluation were carried out in cooperation with the Department of Dynamics, the Institute of Theoretical and Applied Mechanics, the Academy of Science of the Czech Republic. The significant support of Stanislav Pospíšil, Shota Urushadze, Radomil Král and Stanislav Hračov is gratefully acknowledged.

Support was provided from the Ministry of Industry and Trade project no. MPO TIP FR-TI3/654, Czech Grant Agency no. GAČR 103/09/0094 and research project RVO 683782.

REFERENCES

[1] ***Davenport, A. G.,*** Application of statistical concepts of wind loading of structures, *Proceeding,* Institute of Civil Engineers (England), Vol. 19, Paper 6480, pp. 449-472, 1961.

[2] ***Simiu, E., and Scanlan, R. H.,*** Wind effects on structures, *John Wiley and Sons, Inc.*, New York, 1996.

[3] ***Koloušek, V., Pirner, M., Fischer, and O, Náprstek, J.,*** Wind Effects on Civil Engineering *Structures, Academia, Praha 1983, Elsevier*, coed. London 1984.

[4] ***Sparling, B.F., and Davenport, A.G.,*** Three Dimensional Dynamic Response of Guyed Masts to Wind Turbulence, *Meeting of WG4, IASS*, Winchester 1995.

[5] ***Madugula, M. K. S. et al,*** *Dynamics Response of Lattice Towers and Guyed Masts*, ASCE, 2002.

[6] ***ČSN 73 0035,*** *Actions on structures*, 1986.

[7] ***Materazzi, A.L., and Venanzi, I.,*** A simplified approach for the wind response analysis of cable-stayed masts, *Journal of Wind Engineering and Industrial Aerodynamics 95*, 1278-1288, 2007.

[8] ***Lahodný, J.,*** Static and dynamic analysis of towers and masts loaded by wind, *Thesis (PhD)*, Czech Technical University, 2010.

[9] ***EN 1991-1-4,*** *Eurocode 1: Action on structures – Part 1-4: General actions – Wind loads*, 2007.

[10] ***Sparling, B. F., Smith, B. W., and Davenport, A. G.,*** Simplified Dynamics Analysis Methods for Guyed Masts in Turbulent Wind, IASS meeting of WG 4 *(Masts and Towers),* Prague, 1993.

[11] ***EN 1993-3-1,*** *Eurocode 3: Design of steel structures – Part 3-1: Towers, masts and chimneys – Towers and masts,* 2008.

[12] ***Iwatani, Y.:*** Simulation of multidimensional wind fluctuations having any arbitrary power spectra and cross spectra*, J. of Wind Eng. Ind. Aerodyn.*, No. 11, pp. 5-18, 1982.

[13] ***Kármán, T.:*** Progress in the Statistical Theory of Turbulence**,** *Proc. Nat. Acad. Sci. Washington, DC***,** 530-539, 1948

[14] ***Davenport, A.G.:*** The Spectrum of Horizontal Gustiness Near the Ground in High Winds, *J. Royal Meteorol. Soc.,* 87, 194-211, 1961.

[15] ***Kaimal, J.C., Wymgaard, J.C.m Ozimi, Y., and Coté, O.R.:*** Spectral characteristics of surface-layer turbulence**,** *Quartely Journal of Royal Meteorological Society*, Vol. 98, pp. 563-589, 1972.